The Meteoritical Society

Meteoritics & Planetary Science 55, Nr 1, 184–192 (2020)
doi: 10.1111/maps.13426

Wangdaodeite, the $LiNbO_3$-structured high-pressure polymorph of ilmenite, a new mineral from the Suizhou L6 chondrite

Xiande XIE[1,2], Xiangping GU[3*], Hexiong YANG[4], Ming CHEN[2], and Kai LI[5]

[1]Key Laboratory of Mineralogy and Metallogeny, Guangzhou Institute of Geochemistry, Chinese Academy of Sciences, Guangzhou 510640, China
[2]Guangdong Provincial Key Laboratory of Mineral Physics and Materials, Guangzhou 510640, China
[3]School of Geosciences and Info-Physics, Central South University, Changsha, Hunan 410083, China
[4]Department of Geosciences, University of Arizona, 1040 E. 4th Street, Tucson, Arizona 85721-0077, USA
[5]Institute for Materials Microstructure, Central South University, 410083 Changsha, Hunan, PR China
[*]Corresponding author. E-mail: guxp@csu.edu.cn

(Received 12 January 2019; revision accepted 05 November 2019)

Abstract–Wangdaodeite, the shock-induced lithium niobate–structured polymorph of ilmenite, was found in the Suizhou L6 chondrite. It occurs as small irregular particles (2–20 μm in size) inside or adjacent to the shock melt veins. Wangdaodeite coexists in veins with ringwoodite, majorite, and xieite. The chemical formula of wangdaodeite is $FeTiO_3$. The empirical formula is: $(Fe_{0.85}Mg_{0.10}Mn_{0.05})_{\Sigma 1.00}Ti_{0.99}O_3$, which is similar to that of its host ilmenite. The Raman spectra of wangdaodeite display the bands at 174–179, 273–277, 560–567, 738–743 cm^{-1}, which are different to those for ilmenite. TEM images show that ilmenite is composed of polysynthetic-twinned crystals while wangdaodeite is composed of random-oriented nanometric domains sized 20–50 nm. Electron diffraction established wangdaodeite to be trigonal with the lithium niobate structure. Cell parameters are: a = 5.13(1) Å, c = 13.78(1) Å; c/a = 2.69; space group $R3c$; calculated density = 4.72 g cm^{-3}. The P–T conditions for formation of wangdaodeite were estimated to be 20–24 GPa and >1200 °C. The mineral name was approved by the Commission on New Minerals, Nomenclature, and Classification of the International Mineralogical Association (IMA 2016-007). The name is for Daode Wang, Professor at the Guangzhou Institute of Geochemistry, Chinese Academy of Sciences.

INTRODUCTION

A new mineral species, the high-pressure polymorph of ilmenite $FeTiO_3$, has been found in the Suizhou L6 chondrite. It is named wangdaodeite to honor the contributions of Daode Wang, Department of Meteoritics and Cosmochemistry, Guangzhou Institute of Geochemistry, Chinese Academy of Sciences (CAS), to the fields of systematic study of Chinese meteorites in general and Antarctic meteorites in particular. The new mineral and its name have been approved by the Commission on New Minerals and Nomenclature and Classification of the International Mineralogical Association (IMA 2016-007). The type material has been deposited in the collection of the Geological Museum, Guangzhou Institute of Geochemistry, CAS. This paper describes the physical and chemical properties of wangdaodeite, and its single-crystal and polycrystalline electron diffraction and Raman spectroscopic data.

SAMPLE DESCRIPTION AND EXPERIMENTAL METHODS

The Suizhou meteorite is an L6 chondrite containing a few thin shock veins ranging from 0.02 to 0.20 mm in width. The chondritic region of this meteorite consists of olivine, pyroxene, plagioclase, FeNi-metal and troilite, merrillite, chlorapatite, chromite, and ilmenite (Xie et al. 2001, 2011). Ilmenite with a chemical formula of $(Fe_{0.83}Mg_{0.12}Mn_{0.04})_{\Sigma 0.99}Ti_{0.99}O_3$ in a chondritic area occurs in association with

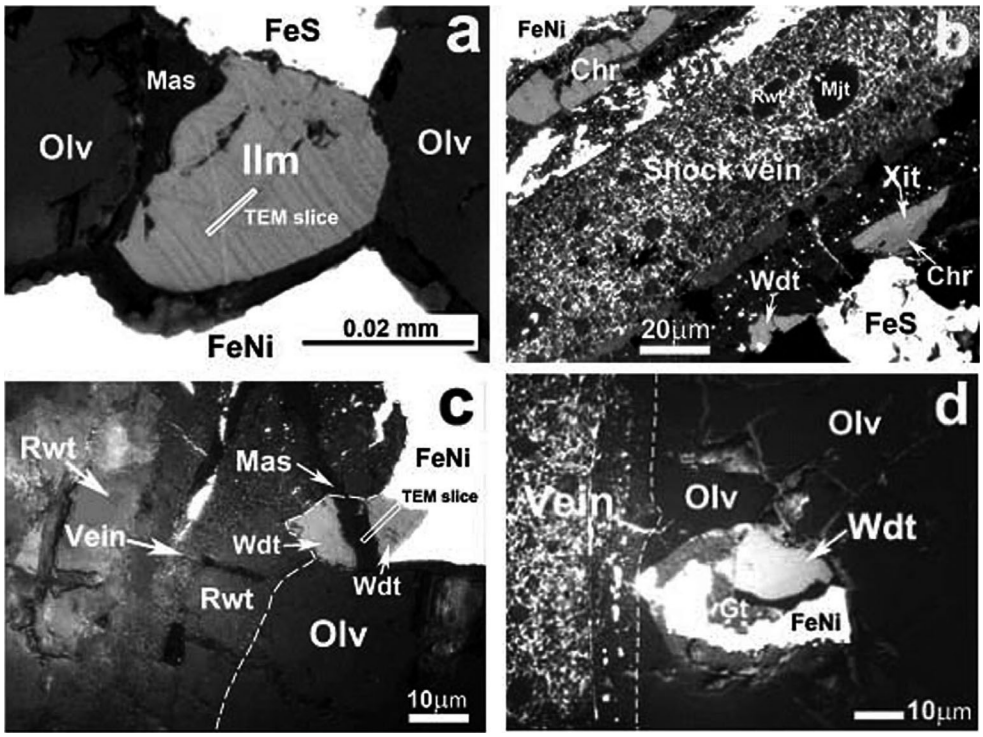

Fig. 1. Photomicrographs showing the occurrences of ilmenite (Ilm) and wangdaodeite (Wdt) in the Suizhou meteorite. a) A polysynthetic-twinned ilmenite grain in unmelted chondritic rock; (b) an irregular wangdaodeite grain on the margin of a shock vein; (c) a wangdaodeite grain partitioned by maskelynite (Mas) in contact with a shock vein; and (d) a wangdaodeite grain in 12 μm apart from a vein. The locations of TEM slices obtained by focused ion beam technique are shown in (a) and (c) and Raman spectra of all the grains of ilmenite and wangdaodeite in the images are measured and shown in Fig. 2. Olv = olivine; Pyx = pyroxene; Mas = maskelynite; Chr = chromite; Rwt = ringwoodite; Mjt = majorite; Xit = xieite; FeNi = FeNi metal; FeS = troilite; Gt = goethite.

FeNi metal and/or troilite as irregular grains less than 20 μm in size (Fig. 1a). Melt veins in this meteorite are full of shock-induced high-pressure minerals, such as ringwoodite, majorite, akimotoite, vitrified perovskite, lingunite, tuite, xieite, $CaFe_2O_4$–structured $FeCr_2O_4$, majorite–pyrope$_{ss}$ (ss-solid solution), magnesiowüstite, and hemleyite (Xie et al. 2001, 2002, 2003, 2011, 2013; Chen et al. 2003, 2004, 2008; Chen and Xie 2015; Bindi et al. 2017).

Polished sections of the Suizhou meteorite were prepared from the vein-bearing fragments. The mineral assemblages were investigated by optical microscopy using a Leica DM2500p microscope and the reflectance was measured with Leica DFC420 CCD using SiC as the standard. A Shimadzu 1720 electron microprobe (EPMA) was used to study the mineral occurrence in backscattered electron mode, and to quantitatively determine the chemical composition of minerals using the wavelength dispersive technique at 15 kV accelerating voltage and beam current of 10 nA. Natural and synthetic phases of well-known compositions were used as standards, such as MgO for Mg, Fe_2O_3 for Fe, TiO_2 for Ti, Al_2O_3 for Al, $MnSiO_3$ for Mn, Cr_2O_3 for Cr, and the data were corrected using a ZAF program attached with the machine. Raman spectra of minerals were recorded with a Horiba Labram Aramis instrument. A microscope was used to focus the excitation beam (532 nm line) to 1 μm wide spots and to collect the Raman signal. Accumulations of the signal lasted 300 s. The laser power was 2 mW. A focused ion (Ga+) beam (FIB) workstation equipped in the FEI Helios Nanolab 600i systems at the Center for Advanced Research of Central South University was used to cut a chip of wangdaodeite and ilmenite in sizes of 10 μm × 7 μm × 0.2 μm, which was mounted onto the molybdenum sample holder and then sliced to a thickness of about 37 nm for TEM observation. TEM and selected area electron diffraction (SAED) were performed using FEI Titan G2 60-300 TEM operated at 300 kV accelerating voltage. The *d*-values of electron diffraction patterns are calibrated using the X-ray diffraction data of ilmenite with the same composition from the Suizhou meteorite (a = 5.0909 Å, c = 14.083 Å). The cell parameters are calculated using the method of Holland and Redfern (1997).

Table 1. Electron microprobe analyses of wangdaodeite and ilmenite (wt%)

Sample	Al_2O_3	TiO_2	FeO	MgO	MnO	V_2O_3	Cr_2O_3	Total
Ilmenite								
SZ-ilm (9)	0.05	54.15	40.89	3.17	1.79	0.30	0.08	100.43
Wangdaodeite								
W-1 (2)	0.10	52.23	39.59	2.44	4.38	0.26	0.05	99.05
W-2 (3)	0.05	53.92	41.00	2.86	2.81	0.27	0.09	101.00
W-3 (2)	0.04	52.85	41.31	2.77	2.29	0.27	0.03	99.56
W-4 (1)	0.02	52.55	41.46	2.69	2.13	0.25	0.02	99.12
W-5 (1)	0.05	52.89	40.85	2.78	2.88	0.29	0.07	99.81
W-6 (1)	—	52.13	41.63	3.03	2.43	—	—	99.22
W-7 (1)	—	52.28	41.50	3.00	2.30	—	—	99.08
Average	0.04	52.69	41.05	2.79	2.74	0.19	0.04	99.54

Numbers in parentheses are numbers of analysis.

OCCURRENCE AND ASSOCIATED MINERALS

Wangdaodeite was found as small irregular particles of 2–20 μm in the Suizhou meteorite. It occurs either inside the shock veins or in the chondritic area adjacent to shock veins. In contrast to the fractured ilmenite grains outside the veins, no microstructures were observed inside the grains of wangdaodeite.

Figure 1b shows a shock vein of 100 μm in width that consists of fine-grained vein matrix with some coarse-grained ringwoodite and majorite fragments. A irregular grain of wangdaodeite about 10 × 20 μm in size occurs on the vein boundary. The associated minerals in the vein are ringwoodite, majorite, and xieite. Figure 1c displays two triangle-shaped wangdaodeite grains of 15 and 12 μm in length, respectively. One is inside the vein and the other is in contact with the vein (Fig. 1c). It seems that these two grains originally belonged to a single grain that was then separated by a maskelynite veinlet of 5 μm wide. Olivine inside the vein has transformed to ringwoodite, while olivine outside the vein remains unchanged.

Several wangdaodeite grains were observed in the chondritic area very close to the shock veins. Figure 1d demonstrates a wangdaodeite grain surrounded by FeNi metal and its weathered product—goethite. The grain is located less than 20 μm apart from the vein.

PHYSICAL PROPERTIES AND CHEMICAL COMPOSITION

The polycrystalline wangdaodeite grains are gray in reflected polarized light (Fig. 1). They are smooth in appearance; no cleavage and parting were observed. Mohs hardness is estimated to be 5–5.5 according to the similar relief to associated ilmenite under a microscope. Streak and luster were not determined because of the polycrystalline nature of the grains. The density calculated from the empirical formula is 4.72 g cm^{3-1}.

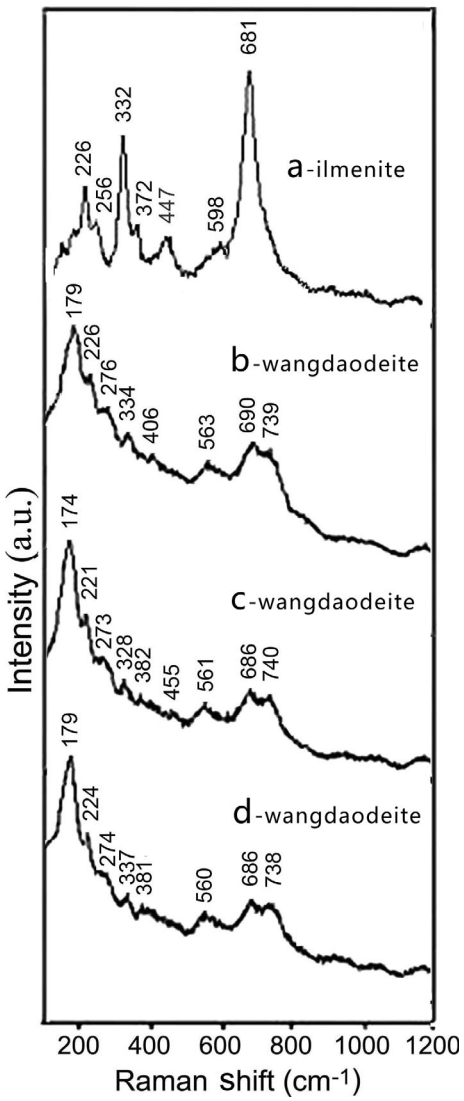

Fig. 2. Raman spectra of ilmenite (a) and wangdaodeite (b, c, and d) in the Suizhou meteorite.

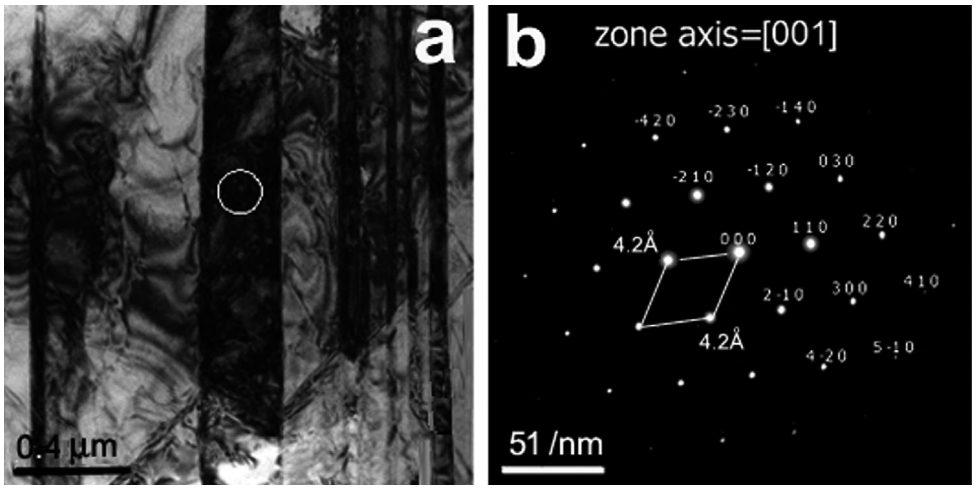

Fig. 3. Bright-field TEM image showing polysynthetic twined crystals of ilmenite (a), and its well-resolved electron diffraction pattern along the zone axis [0 0 1] (b).

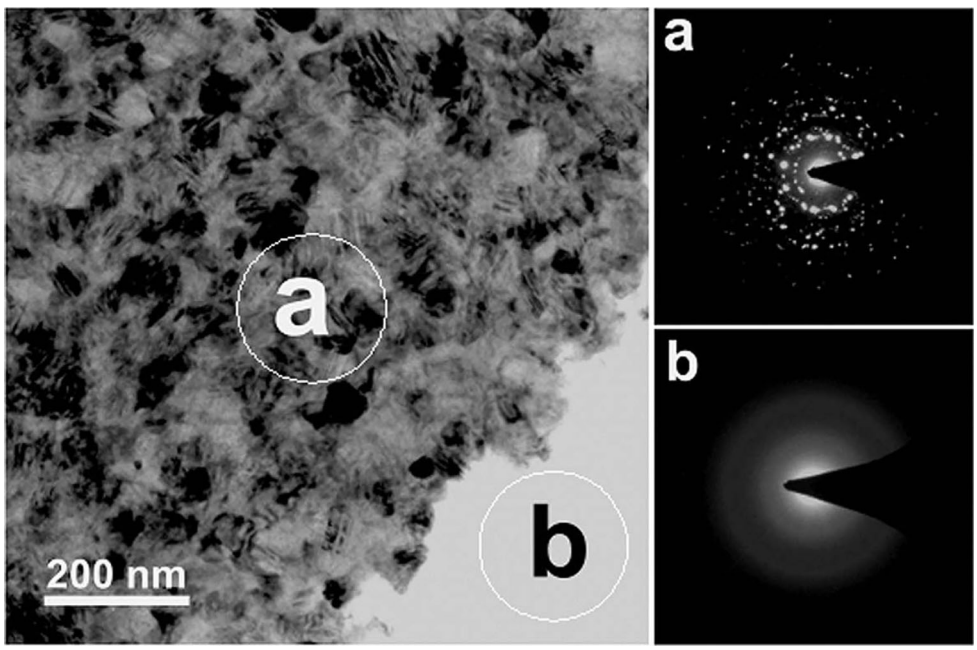

Fig. 4. Bright-field TEM image showing the nanometric crystals of wangdaodeite (a) and glassy maskelynite (b), and the SAED pattern of these two phases. Note the polycrystalline nature of wangdaodeite.

The reflectance data of wangdaodeite are: 21.0–18.7% at 470 nm, 19.9–17.9% at 546 nm, 20.1–18.0% at 589 nm, 20.4–18.3% at 650 nm.

The results of electron microprobe analyses of wangdaodeite and ilmenite in the Suizhou meteorite are listed in Table 1. On the basis of 3 O atoms per formula unit, the empirical formulas for wangdaodeite and ilmenite can be written as $(Fe_{0.85}Mg_{0.10}Mn_{0.05})_{\Sigma 1.00}Ti_{0.99}O_3$ and $(Fe_{0.83}Mg_{0.12}Mn_{0.04})_{\Sigma 0.99}Ti_{1.00}O_3$, respectively. The ideal chemical formula for both wangdaodeite and ilmenite is $FeTiO_3$. Evidently, wangdaodeite and its precursor ilmenite are almost identical in composition.

RAMAN SPECTROSCOPY

Raman spectra measured on three wangdaodeite grains are shown in Figs. 2b–d. They are apparently different from that of the Suizhou ilmenite (Fig. 2a). For wangdapodeite, seven bands at 174–179, 273–276, 328–337, 381–382, 455, 560–563, 738–740 cm^{-1} were

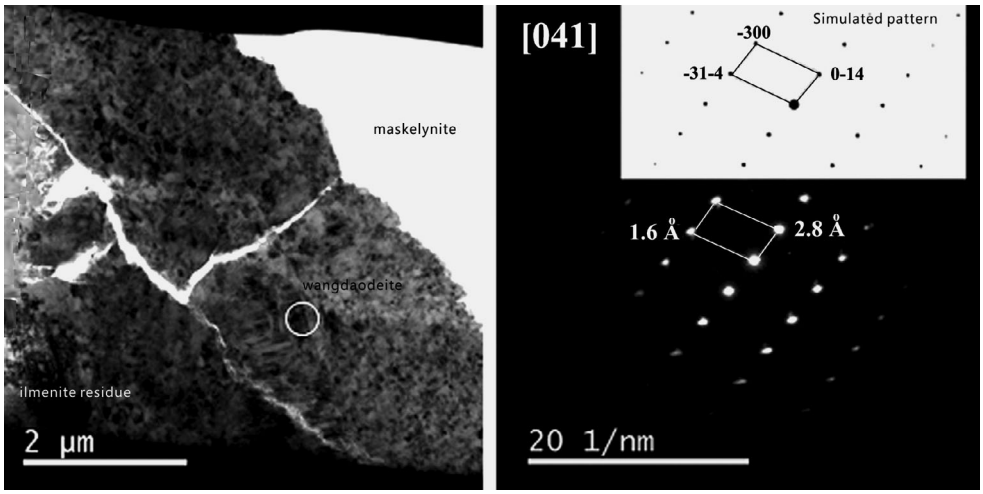

Fig. 5. Bright-field TEM image showing a single crystal of wangdaodeite in the nanometric matrix, and the electron diffraction pattern along the zone axis [0 4 1] embedded with simulated pattern. Note the ilmenite residue toward the outer boundary of the agglomerate

observed. The additional three peaks at 221–226, 406, and 686–690 cm^{-1} do not belong to wangdaodeite but to the relics of precursor ilmenite.

The Raman spectra of wangdaodeite are similar to those of synthesized $LiNbO_3$-type $MnTiO_3$ (Ko et al. 1989; Wu et al. 2011). Barnert et al. (2015) reported that $ZnTiO_3$ also behaves similarly as $FeTiO_3$ and $MnTiO_3$ at high pressure and high temperature, and the Raman spectrum of synthetic $LiNbO_3$-type $ZnTiO_3$ is also similar to that of wangdaodeite. Since the Raman spectrum of $LiNbO_3$-type polymorph of $MnTiO_3$ is more similar to that of $LiNbO_3$-type polymorph of $FeTiO_3$ (Linton et al. 1999), we assume that all these three grains are mainly composed of wangdaodeite mixed with a little remain of ilmenite.

TRANSMISSION ELECTRON MICROSCOPY

A wangdaodeite grain on Fig. 1c and an ilmenite grain on Fig. 1a were subjected to transmission electron microscopic observations after thinning with FIB technique. Figure 3a shows a bright-field TEM image of polysynthetic-twinned ilmenite. This image shows clear lamellar structure with lamellae width of 50–200 nm and complex waveform fine textures in the image. Figure 3b is the SAED pattern (circle in Fig. 3a), which shows a typical hexagonal close-packed lattice.

The bright-field TEM images of wangdaodeite are shown in Figs. 4a and 5a. Much more complex fabrics are displayed in these images, which are composed of randomly oriented nanometric domains sized 20–50 nm and lack the regular polysynthetic lamellae observed in ilmenite. The electron diffraction patterns of polycrystalline material (Fig. 4a) lacks the dots with d = 4.2 Å, which are present in the pattern of ilmenite (Fig. 3b). The d-values of the electron diffraction data are calibrated with the XRD data of ilmenite from the Suizhou meteorite and listed in Table 2. The strong diffraction lines for wangdaodeite are 2.72 (100), 2.56 (89), 3.75 (72), 1.86 (59), 2.23 (57), 1.51 (44), 1.62 (41) Å. The cell parameters are calculated to be a = 5.13(1) Å and c = 13.78(1) Å, c/a = 2.69. The c/a ratio is different from that of ilmenite but in accord with that of synthetic $LiNbO_3$-type $FeTiO_3$ (Wu et al. 2010). Wangdaodeite has a calculated density of 4.72 g cm^{-3},

Table 2. Polycrystal electron diffraction data of wangdaodeite

I/*I*0	*d*obs. (Å)	*d*calc. (Å)	*h*	*k*	*l*
72	**3.75**	**3.73**	**1**	**0**	**−2**
100	**2.72**	**2.72**	**1**	**0**	**4**
89	**2.56**	**2.56**	**2**	**−1**	**0**
16	2.29	2.30	0	0	6
57	**2.23**	**2.24**	**2**	**−1**	**3**
14	2.10	2.11	2	0	2
59	**1.86**	**1.86**	**2**	**0**	**−4**
25	1.72	1.71	2	−1	6
41	1.62	**1.61**	**1**	**0**	**−8**
44	**1.51**	**1.51**	**3**	**−1**	**4**
38	**1.48**	**1.48**	**3**	**0**	**0**
13	1.36	1.36	2	0	8
27	1.31	1.32	1	0	10
38	1.28	1.28	4	−2	0
6	1.25	1.24	3	0	−6
23	1.20	1.20	3	−1	−8

The data are obtained from the polycrystal electron diffraction pattern in Fig. 4, the refined unit cell parameters are a = 5.13(1) Å, c = 13.78(1) Å, V = 316.6(1) Å3 using the method of Holland and Redfern (1997). Bold lines are the eight strongest peaks.

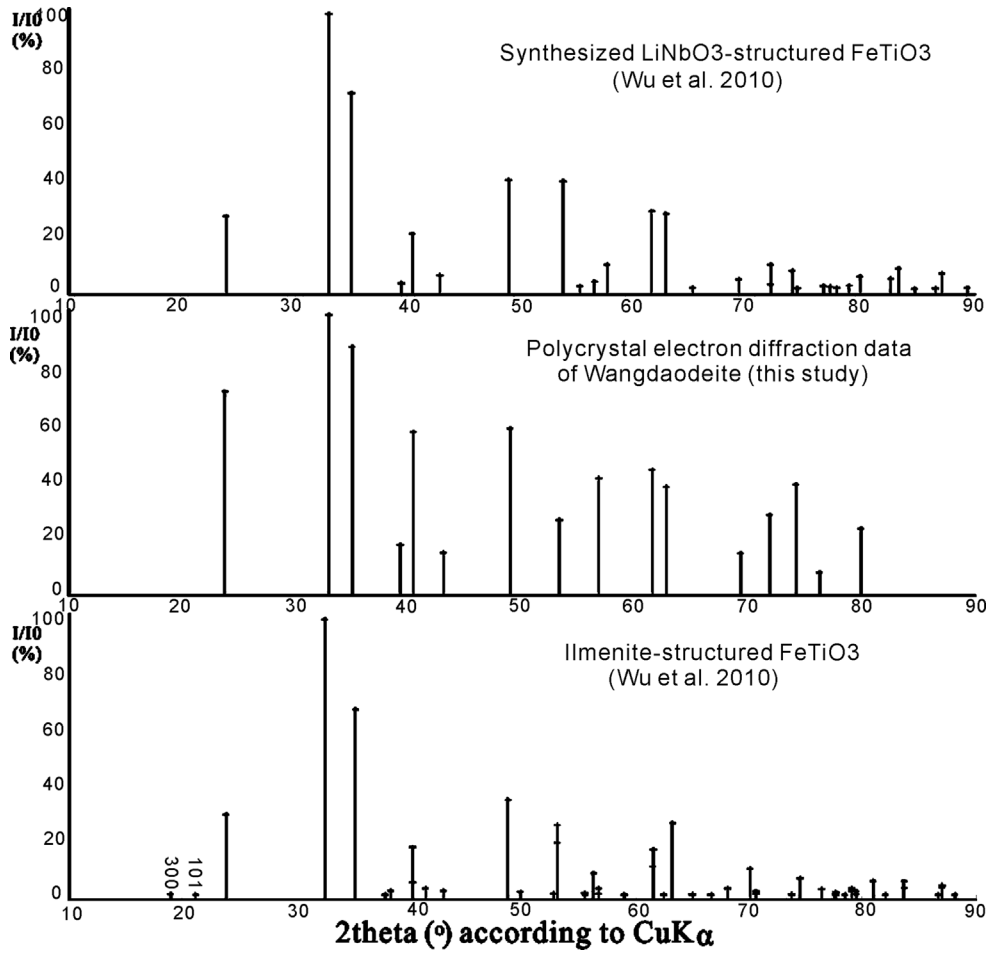

Fig. 6. X-ray powder diffraction patterns of synthetic $LiNbO_3$-structured $FeTiO_3$ (a), polycrystal electron diffraction pattern of wangdaodeite (b), and ilmenite-structured $FeTiO_3$ (c). Note the reflections of (003) (d = 4.82 Å), (101) (d = 4.22 Å) of ilmenite are absent in wangdaodeite, in addition to different c/a ratios (2.690 for wangdaodeite and 2.768 for ilmenite).

which is 4% denser than its precursor ilmenite (4.54 g cm^{-3}). Figure 4a also shows the occurrence of maskelynite, a glassy phase of plagioclase, which is confirmed by the diffused diffraction rings on the SAED pattern (Fig. 4b). The boundary line between maskelynite and wangdaodeite is uneven.

It should be pointed out that residual ilmenite was observed toward the outer part of the grain of wangdaodeite nanometric agglomerate in Fig. 5. This is consistent with the results of Raman spectroscopic analyses.

DISCUSSION

Crystal Structure

The crystal structure of synthetic $LiNbO_3$-type $FeTiO_3$ determined by Leinenweber et al. (1991) and Wu et al. (2010) is very similar to that of ilmenite (R-3) with the same hexagonal-close-packed lattice. Figure 6 and 7 show the comparison of powder XRD patterns and the partial structures of $LiNbO_3$-type $FeTiO_3$ and ilmenite phase reported by Wu et al. (2010). From Fig. 7, we can see that the structure of both $LiNbO_3$-type $FeTiO_3$ and ilmenite consists of corner-linked TiO_6 octahedra, but the adjacent octahedral layers for the $LiNbO_3$-type $FeTiO_3$ are rotated relative to one another compared with the ilmenite structure (Fig. 7a). In contrast, the TiO_6 octahedra in the ilmenite phase share edges (Fig. 7b), which indicates that bonds must be broken in the ilmenite for the transition to $LiNbO_3$-structure. Wu et al. (2010) pointed out that although the structures of $LiNbO_3$-type $FeTiO_3$ and ilmenite are very similar, the axial ratio of c/a is an effective criterion to distinguish $R3c$ $LiNbO_3$-type $FeTiO_3$ (i.e., wangdaodeite) from R-3 ilmenite, because ilmenite exhibits consistently larger values ($2.765-0.003 \times P$, where P is pressure in GPa) than $LiNbO_3$-type $FeTiO_3$ ($2.683-0.002 \times P$). Our determined axial c/a ratio for

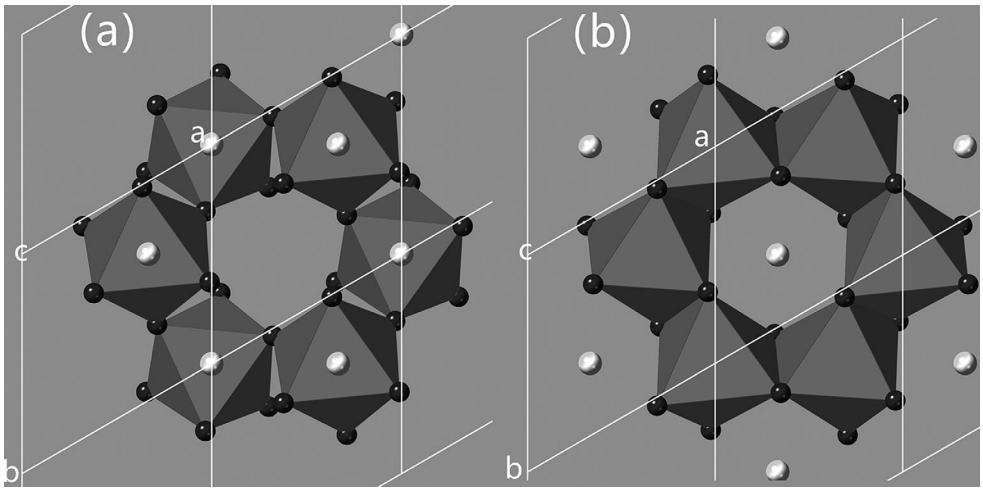

Fig. 7. Comparison of the partial structures of (a) the lithium-niobate structured phase of $FeTiO_3$ (wangdaodeite) and (b) the ilmenite phase. View along [001] of these two phases. The TiO6 octahedra are shown in gray, and the iron and oxygen atoms are indicated as gray and black spheres, respectively (after Wu et al. 2010).

wangdaodeite is 2.694, in accordance with the conclusion by Wu et al. (2010).

Origin

The identical composition of wangdaodeite and its precursor ilmenite in the Suizhou meteorite implies that this new phase formed from ilmenite through an isochemical phase transition in solid state under shock-produced high pressure and high temperature. Pressure-induced phase transition of $FeTiO_3$ has been investigated by various experimental methods and theoretical calculations (Liu 1975; Syono et al. 1981; Mehta et al. 1994; Wilson et al. 2005; Ming et al. 2006; Wu et al. 2009a, 2009b, 2010). Three polymorphs of $FeTiO_3$ have been observed experimentally: ilmenite, the lithium niobate structure, and the perovskite structure. High-pressure experiments by Syono et al. (1981) revealed a phase transition of $FeTiO_3$ from the ilmenite structure to a hexagonal structure. This hexagonal structure was then determined to be the lithium niobate structure (Ko and Prewitt 1988; Leinenweber et al. 1991). Leinenweber et al. (1991) reported that this $LiNbO_3$-structured $FeTiO_3$ transforms to an orthorhombic perovskite-type polymorph at 16 GPa, but during quenching this perovskite-type phase reverted to the lithium niobate structure. Hence, we assume that wangdaodeite in the Suizhou meteorite might be a retrogressive product that results from the perovskite-type phase during decompression.

P–T Conditions

Static high-pressure and high-temperature experiments have revealed that the ilmenite transforms to perovskite type at 20 GPa (Ming et al. 2006; Wu et al. 2009a), but during quenching, this perovskite-type $FeTiO_3$ reverted to the $LiNbO_3$-structure at 16 GPa (Leinenweber et al. 1991). Linton et al. (1997) reported that a complete Fe-Mg solid solution was revealed in lithium niobate and perovskite structures in titanates at high pressures and temperatures, and a high-pressure $MgTiO_3$ phase with the lithium niobate structure was recovered after synthesis at 21 GPa and 1200 °C. Dubrovinsky et al. (2009) reported an occurrence of tiny grains of $LiNbO_3$-type $FeTiO_3$ in the Ries crater, Germany, and suggested a shock pressure up to at least 20 GPa. Hence, we assume that the *P–T* conditions for formation of lithium niobate structure from ilmenite structure can be estimated as 16–21 GPa and 1200 °C.

In Suizhou shock veins, wangdaodeite is associated with coarse-grained ringwoodite and majorite, and fine-grained garnet and magnesiowüstite (Fig. 1b). Based on the phase diagram of Agee et al. (1995), such high-pressure mineral assemblages constrain the pressure and temperature regime of up to 24 GPa and 1900–2000 °C for the Suizhou shock vein (Xie et al. 2011). The presence of maskelynite in the Suizhou unmelted chondritic rock implies that this rock experienced a *P–T* regime of 20–22 GPa and 1000 °C (Xie et al. 2011). It is clear that there exists a sharp temperature gradient from the shock vein (1900–2000 °C) to the unmelted chondritic rock (1000 °C) in the Suizhou meteorite. It appears, therefore, that the phase transformation from ilmenite to perovskite-type and then to wangdaodeite could take place inside the shock vein, or in the chondritic area close to the shock veins where the *P–T* conditions (20–24 GPa and >1200 °C) should have been available for such transformation.

IMPLICATIONS

The finding of wangdaodeite is of important significance in mineralogy of the Earth's mantle because it is believed to be one of the high-pressure phases stable in the lower part of the mantle's transition zone (Tomioka and Fujino 1999; Chen and Xie 2015). Wangdaodeite can be used as an important indicator of mineralogical or petrological processes, such as a geobarometer for $FeTiO_3$-bearing rocks that may occur in ultrahigh-pressure metamorphic belts, in naturally shocked rocks of impact craters, or in ultramafic rocks being carried up from the deep mantle/interior of terrestrial and extraterrestrial bodies. Therefore, the relationship of ilmenite, lithium niobate structure, and perovskite structure for ABO_3 compounds is of fundamental interest in high-pressure crystal chemistry and of significance in the Earth science (Wu et al. 2011). In the field of materials science, $LiNbO_3$-type $FeTiO_3$ has recently been confirmed to be a multiferroic material where ferroelectricity and weak ferromagnetism coexist at low temperatures (Varga et al. 2009).

Acknowledgments—This study was supported by the National Natural Science Foundation of China under grant no. 41172046 and the Guangdong Provincial Key Laboratory of Mineral Physics and Materials. The authors are grateful to Prof. Wu Xiang of Peking University, China, and Prof. Leonid Dubrovinsky of University of Bayreuth, Germany, for instructive discussions. We wish to thank to Dr. Zhou Tao and Dr. Yan Ning for their help in Raman spectroscopic and transmission electron microscopic analyses, respectively.

Editorial Handling—Dr. Alexander Ruzicka

REFERENCES

Agee C. B., Li J., Shannon M. C., and Circone S. 1995. Pressure-temperature phase diagram for Allende Meteorite. *Journal of Geophysical Research* 100:17,725–17,740.

Barnert T., Ruiz-Fuertes J., Bayarjargal L., and Winkler B. 2015. Synthesis and high (pressure, temperature) stability of $ZnTiO_3$ polymorph studied by Raman spectroscopy. *Solid State Sciences* 43:53–58.

Bindi L., Chen M., and Xie X. D. 2017. Discovery of the Fe-analogue of akimotoite in the shocked Suizhou L6 chondrite. *Scientific Reports* 7:42674.

Chen M. and Xie X. 2015. Shock-produced akimotoite in the Suizhou L6 chondrite. *Science China Earth Sciences* 58:876–880.

Chen M., Shu J., Mao H. K., Xie X., and Hemley R. J. 2003. Natural occurrence and synthesis of two new postspinel polymorphs of chromite. *Proceedings of the National Academy of Sciences* 100:14,651–14,654.

Chen M., Xie X., and E1 Goresy A. 2004. A shock-produced (Mg, Fe)SiO_3 glass in the Suizhou meteorite. *Meteoritics & Planetary Science* 39:1797–1808.

Chen M., Shu J., and Mao H. K. 2008. Xieite, a new mineral of high-pressure $FeCr_2O_4$ polymorph. *Chinese Science Bulletin* 53:3341–3345.

Dubrovinsky L., El Goresy A., Gillet P., Wu X., and Simionivici A. 2009. A novel natural shock-induced high-pressure polymorph of $FeTiO_3$ ilmenite with the Li-niobate structure from the Ries crater, Germany. *Meteoritics & Planetary Science* 44:A64.

Holland T. and Redfern S. 1997. Unit cell refinement from powder diffraction data: The use of regression diagnostics. *Mineralogical Magazine* 61:65–77.

Ko J. and Prewitt C. T. 1988. High-pressure phase transition in $MnTiO_3$ from the ilmenite to the $LiNbO_3$ structure. *Physics and Chemistry of Minerals* 15:355–362.

Ko J., Brown N. E., Navrotsky A., Prewitt C. T., and Gasparik T. 1989. Phase equilibrium and calorimetric study of the transition of MnTiO3 from the ilmenite to the lithium niobate structure and implications for the stability field of perovskite. *Physics and Chemistry of Minerals* 16:727–733.

Leinenweber K., Utsumi W., Tsuchida Y., Yagi T., and Kurita K. 1991. Unquenchable high-pressure perovskite polymorphs of $MnSnO_3$ and $FeTiO_3$. *Physics and Chemistry of Minerals* 18:244–250.

Linton J. A., Fei Y. and Navrotsky A. 1997. Complete Fe-Mg solid solution in lithium niobate and perovskite structures in titanates at high pressures and temperatures. *American Mineralogist* 82:639–642.

Linton J. A., Fei Y., and Navrotsky A. 1999. The $MgTiO_3$-$FeTiO_3$ join at high pressure and temperature. *American Mineralogist* 84:1595–1603.

Liu H. 1975. High-pressure phase transformations and compressions of ilmenite and rutile: I. Experimental results. *Physics of the Earth and the Planetary Interior* 10:167–176.

Mehta A., Leinenweber K., Navrotsky A., and Akaogi M. 1994. Calorimetric study of high pressure polymorphism in $FeTiO_3$: Stability of the perovskite phase. *Physics and Chemistry of Minerals* 21:207–212.

Ming L. C., Kim Y. H., Uchida T., Wang Y., and Rivers M. 2006. In situ X-ray diffraction study of phase transitions of $FeTiO_3$ at high pressures and temperatures using a large-volume press and synchrotron radiation. *American Mineralogist* 91:120–126.

Syono Y., Takei H., Goto T., and Ito A. 1981. Single crystal X-ray and Mössbauer study of shocked ilmenite to 80 GPa. *Physics and Chemistry of Minerals* 7:82–87.

Tomioka N. and Fujino K. 1999. Akimotoite, (Mg, Fe)SiO_3, a new silicate mineral of the ilmenite group in the Tenham chondrite. *American Mineralogist* 84:267–271.

Varga T., Kumar A., Vlahos E., Denev S., Park M., Hong S., Sanehira T., Wang Y., Fennie C. J., Streiffer S. K., Ke X., Schiffer P., Gopalan V., and Mitchell J. F. 2009. Coexistence of weak ferromaganetism and ferroelectricity in the high pressure $LiNbO_3$-type phase of $FeTiO_3$. *Physical Review Letters* 103:047601-14.

Wilson N. C., Russo S. P., Muscat J., and Harrison N. M. 2005. High-pressure phase of $FeTiO_3$ from first principles. *Physical Review B* 72:024110-18.

Wu X., Steinle-Neumann G., Narygina O., Kantor I., McCammon C., Pascarelli S., Aquilanti G., Prakapenka V., and Dubrovinsky L. 2009a. Iron oxidation state of $FeTiO_3$ under high pressure. *Physical Review B* 79:094106-17.

Wu X., Steinle-Neumann G., Narygina O., Kantor I., McCammon C., Prakapenka V., Swamy V., and Dubrovinsky L. 2009b. High-pressure behavior of perovskite: $FeTiO_3$ dissociation into (Fe1−δ, Tiδ)O and Fe1+δTi_2−δO_5. *Physical Review Letters* 103:065503-1-4.

Wu X., Steinle-Neumann G., Narygina O., McCammon C., and Dubrovinsky L. 2010. In-situ high-pressure study of $LiNbO_3$-type $FeTiO_3$: X-ray diffraction and Mössbauer spectroscopy. *High Pressure Research* 30:395–405.

Wu X., Qin S., and Dubrovinsky L. 2011. Investigation into high-pressure behavior of $MnTiO_3$: X-ray diffraction and Raman spectroscopy with diamond anvil cells. *Geoscience Frontiers* 2:107–114.

Xie X., Chen M., and Wang D. 2001. Shock-related mineralogical features and P-T history of the Suizhou L6 chondrite. *European Journal of Mineralogy* 13:1177–1190.

Xie X., Minitti M. E., Chen M., Mao H. K., Wang D., Shu J., and Fei Y. 2002. Natural high-pressure polymorph of merrillite in the shock vein of the Suizhou meteorite. *Geochimica et Cosmochimica Acta* 66:2439–2444.

Xie X., Minitti M. E., Chen M., Wang D., Mao H. K., Shu J., and Fei Y. 2003. Tuite, γ-$Ca_3(PO_4)_2$, a new high pressure phosphate mineral. *European Journal of Mineralogy* 15:1001–1005.

Xie X., Sun Z., and Chen M. 2011. The distinct morphological and petrological features of shock melt veins in the Suizhou L6 meteorite. *Meteoritics & Planetary Science* 46:459–469.

Xie X., Zhai S., Chen M., and Yang H. 2013. Tuite, γ-$Ca_3(PO_4)_2$, formed from chlorapatite decomposition in the shock vein of the Suizhou L6 chondrite. *Meteoritics & Planetary Science* 48:1515–1523.